
Observations of Solar-Wind-Magnetosphere Coupling at the Earth's Magnetopause [and Discussion]

C. J. Farrugia, S. Schwartz, M.J. Rycroft and D. A. Bryant

Phil. Trans. R. Soc. Lond. A 1989 **328**, 57-77
doi: 10.1098/rsta.1989.0024

Email alerting service

Receive free email alerts when new articles cite this article - sign up in the box at the top right-hand corner of the article or click [here](#)

To subscribe to *Phil. Trans. R. Soc. Lond. A* go to: <http://rsta.royalsocietypublishing.org/subscriptions>

Observations of solar-wind–magnetosphere coupling at the Earth's magnetopause

BY C. J. FARRUGIA

Department of Physics, Imperial College, London SW7 2AZ, U.K.

Significant observations have been made with the *Active Magnetospheric Particle Tracer Explorers* data-set on the signatures of reconnection, thought to be the major process responsible for the coupling of the solar wind to the terrestrial magnetosphere. We review results reached by some of these studies. Recent theoretical ideas on reconnection at the terrestrial magnetopause, both time-independent and time-dependent, are also briefly discussed. Two data examples from the *International Sun–Earth Explorer* mission are revisited and interpreted in the light of these newer developments.

1. INTRODUCTION

In the late 1970s, analysis of the extensive *International Sun–Earth Explorer (ISEE)* 1 and 2 data-sets provided observational confirmation of what is thought to be the major process coupling the solar wind to the Earth's magnetosphere and thereby driving large-scale plasma motion inside the magnetosphere. This is magnetic field-line reconnection between the solar and terrestrial fields, first suggested by Dungey (1961). Two types of observational signatures of reconnection were found in the data: one interpreted as a sporadic and intermittent variant and another interpreted as reconnection occurring in a quasi-steady fashion.

After a brief introduction to the signatures in spacecraft data relating to these two forms, the first part of this article is devoted to a review of some of the advances made in these areas of research with the *Active Magnetospheric Particle Tracer Explorers (AMPTE)* data-set with its superior temporal resolution and routine availability of particle data, also at good resolution. We then briefly discuss recent advances in the theory of time-independent reconnection in a fluid-theoretical approach. We shall illustrate the application of this theory to a famous reconnection example and compare theoretical predictions with what is observed. Following a short account of theoretical ideas on reconnection in the time-dependent case, we shall finally discuss another data example. This latter serves a dual purpose: firstly, to bring the forms of observational signatures for reconnection under a common banner and, secondly, to illustrate features in the time-dependent situation which a thorough-going theory might be expected to model. Here we anticipate a little, as a rigorous, general theory of time-dependent reconnection appropriate in a magnetopause context is not yet available. The last two data examples mentioned are the joint work of Imperial College, the Institut für Weltraumforschung in Graz, the State University of Leningrad, the Institut für Extraterrestrische Physik, Garching, and the University of California at Los Angeles. The last two examples are both from *ISEE* spacecraft data, but an application of the time-independent theory mentioned earlier to parameter régimes typical of the magnetopause has been done and applications to the *AMPTE* data-set are envisaged.

2. OBSERVATIONAL SIGNATURES

2.1. General

When studying magnetic field data related to magnetopause crossings, it is usual to present the magnetic field vectors in boundary normal coordinates introduced by Russell & Elphic in 1978 (figure 1). One determines first the vector N , the normal to the notional magnetopause (there are several methods). L is defined such that the NL -plane shown in figure 1 contains the geocentric solar magnetospheric (GSM) z -axis and L points northwards along the magnetopause, while M completes the right-handed triad and points westwards.

Let us imagine an outbound crossing of the dayside magnetopause when the magnetosheath and magnetosphere fields have antiparallel B_L components (figure 2). Two field components are shown here, B_L and B_N . As we move away from the Earth, we encounter bipolar variations in the normal field component, shown here as a positive followed by a negative excursion. Such signatures are called flux transfer events (FTEs). By definition, FTEs are magnetic signatures and they were first discovered by Russell & Elphic (1978). The B_N variation is seen accompanied by changes in the B_L component. FTEs are observed up to *ca.* $1 R_E^\dagger$ away from the magnetopause. This latter is the current layer separating the sheath from the magnetosphere and we can identify it in figure 2 as the region in which B_L reverses sign from a consistently positive to a consistently negative orientation. As the magnetopause is crossed, jetting plasma is seen; this is what we shall hereafter call the high-speed flow region (HSFR). On the sheath side of the magnetopause, rapid, short-duration excursions of the B_L component are seen. They are associated with clear B_N activity which is, however, not manifestly FTE-like. These we call ' B_L spikes'. Once inside the sheath, further FTEs are seen, of the same polarity as those in the magnetosphere. This hypothetical magnetopause crossing therefore has three signatures, HSFRs, FTEs and B_L spikes, which we also see in real spacecraft data. We shall now comment on each of these in turn.

2.2. High-speed flow regions

By definition, one looks for accelerated plasma flows at the magnetopause. The presence of such flows is a long-predicted feature of fluid models of reconnection. In their study (Paschmann *et al.* 1979; Sonnerup *et al.* 1981; Gosling *et al.* 1982), one typically identifies the magnetopause with a large-amplitude Alfvén wave and tests the appropriate jump conditions on the velocity and magnetic fields across such a wave in an anisotropic plasma (Hudson 1970). These relations may be written as

$$[\mathbf{v}_t] = A[\mathbf{B}_t\rho] \quad (1)$$

(momentum conservation) and
$$[\rho(1-\alpha)] = 0 \quad (2)$$

(mass conservation), where
$$A = \{(1-\alpha_1)\rho_1/\mu_0\}^{\frac{1}{2}}$$

(pressure anisotropy factor). $[F_t]$ denotes the tangential jump of the quantity F across the magnetopause. The suffix '1' indicates values at a reference 'point' (interval, in practice) in the sheath. Equation (1) forms the basis of the so-called 'stress balance' test. There is also an energy balance test (Paschmann *et al.* 1985), which relates, with some simplifications, the electromagnetic energy input per unit area in the magnetopause rest frame to the increases in kinetic energy and enthalpy of the plasma and the energy removed as heat flux.

$\dagger R_E = 6.37 \times 10^6$ m.

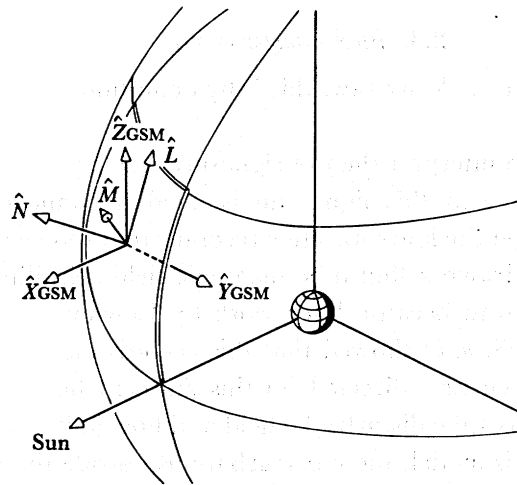


FIGURE 1. The boundary normal coordinate system LMN .

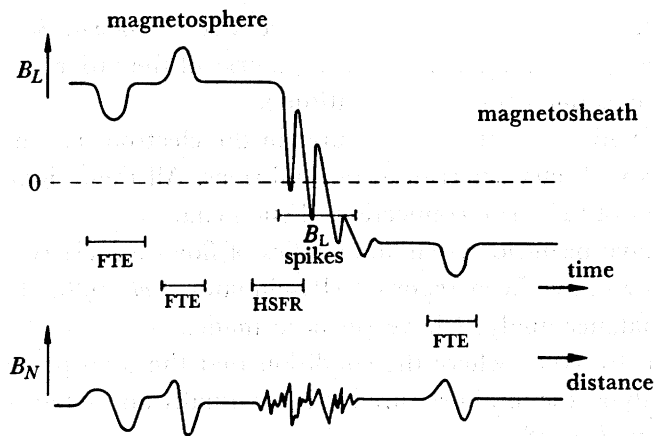


FIGURE 2. A hypothetical crossing of the terrestrial magnetopause showing the types of reconnection signatures encountered. These are (1) HSFRs at the magnetopause; (2) FTEs on both sides of the magnetopause and at the magnetopause itself; (3) B_L spikes on the sheath side of the magnetopause.

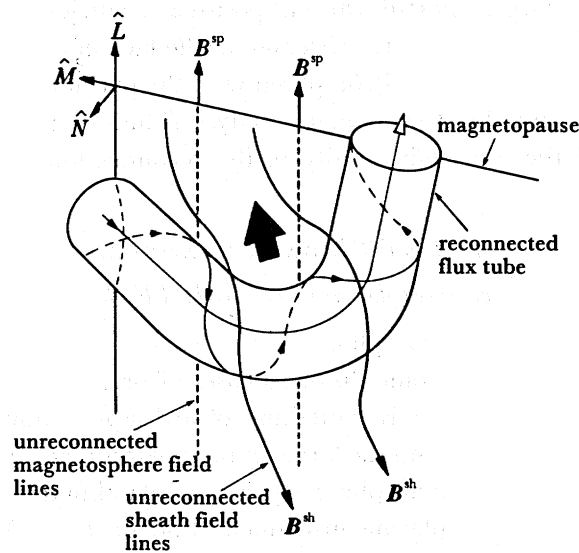


FIGURE 3. A schematic showing a reconnected flux tube moving northwards after reconnecting near the subsolar point, for example (view from the sun). This cartoon, with some later important additions, is that advanced by Russell & Elphic (1978) to account for FTE signatures.

2.3. Flux transfer events

The second signature is the FTE. As we saw, this is by definition a signature in the magnetic field data.

A cartoon much in vogue to interpret the FTE signature was proposed by Russell & Elphic in 1978 (see figure 3). We see in this figure an isolated, reconnected flux tube moving northwards, as indicated by the thick arrow, after reconnection somewhere near the subsolar point, for example. We have drawn a flux tube magnetic field spiralling about the flux tube axis. We have added this feature because later work by Cowley (1982), Paschmann *et al.* (1982) and Saunders *et al.* (1984*a, b*) showed that this accords more with observations. This implies an axial field-aligned current directed, in this ambient field configuration, into the ionosphere. As it moves, the flux tube disturbs the field and flow in its vicinity. This is the field-line draping region. Within this model, these perturbations outside the reconnected flux tube can be understood from theoretical work by Southwood (1985) and Farrugia *et al.* (1987*a*).

FTEs are seen often during magnetopause crossings when the sheath B_L component is negative. Surveys (Berchem & Russell 1984; Rijnbeek *et al.* 1984*a*; Southwood *et al.* 1986) have indicated an average recurrence rate for large FTEs of the order of 1 every 10 min with a tendency to decrease as one goes down in latitude.

FTEs are associated with a variety of signatures in the electron, ion and energetic particle populations as well as with characteristic wave emissions. All these signatures are consistent with the interpretation of FTEs as reconnection phenomena.

Up to now there have been no systematic studies of flows associated with FTEs, although accelerated plasma flows have been reported (Paschmann *et al.* 1982; Farrugia *et al.* 1988). No conclusive stress balance analyses have yet been made.

In contradistinction to HSFs, where the condition that the total pressure be constant is a prerequisite of the analysis, the total pressure in FTEs is usually above background (Paschmann *et al.* 1982; Farrugia *et al.* 1988).

2.4. B_L spikes

The B_L spikes, our last reconnection signature, have not been explicitly studied (but see Rijnbeek 1984). These large, short-duration, positive excursions of the northward field component can be studied neither as FTEs (because of the lack of a B_N signature) nor as HSFs, because the rapid variability of the field compared with the plasma instrument's resolution has generally precluded a meaningful stress balance analysis. They are none the less very important to an understanding of the underlying unity of the reconnection signatures, as we explain below.

3. AMPTE DATA EXAMPLES

3.1. High-speed flow regions: AMPTE observations

We now discuss AMPTE data examples.

With the ISEE spacecraft pair, some 20 or so cases of HSFs for the period 1977–79 were studied quantitatively. This number is something of a disappointment in view of the large number of magnetopause crossings and the large amount of indirect evidence that reconnection plays an important role in magnetosphere dynamics. Paschmann *et al.* (1986) used the improved time resolution of the plasma instrumentation on the AMPTE-IRM (*Ion Release Module*) spacecraft to readdress the important question of occurrence frequency of high-speed

flows in magnetopause encounters. The major result of this investigation was to drastically upgrade this occurrence frequency.

Paschmann *et al.* examined those passes in 1984 characterized by large magnetic shear (21 passes out of 40 with field shears between 60° and 180°). It was found that on about half of them accelerated plasma flows were observed. These often lasted just a few tens of seconds, that is, for periods typically shorter than the three-dimensional *ISEE* plasma measurement resolution. A number of these cases were analysed in detail and they were found to satisfactorily obey stress balance and energy balance predictions.

To illustrate this, we give an example from the inbound pass on 4 September 1984, famous among other things for a very long encounter with the magnetopause and boundary layer lasting *ca.* 20 min. This example was also studied by Johnstone *et al.* (1986).

Figure 4 is the data overview: two hours spanning *ca.* $3 R_E$ moving earthwards, southerly

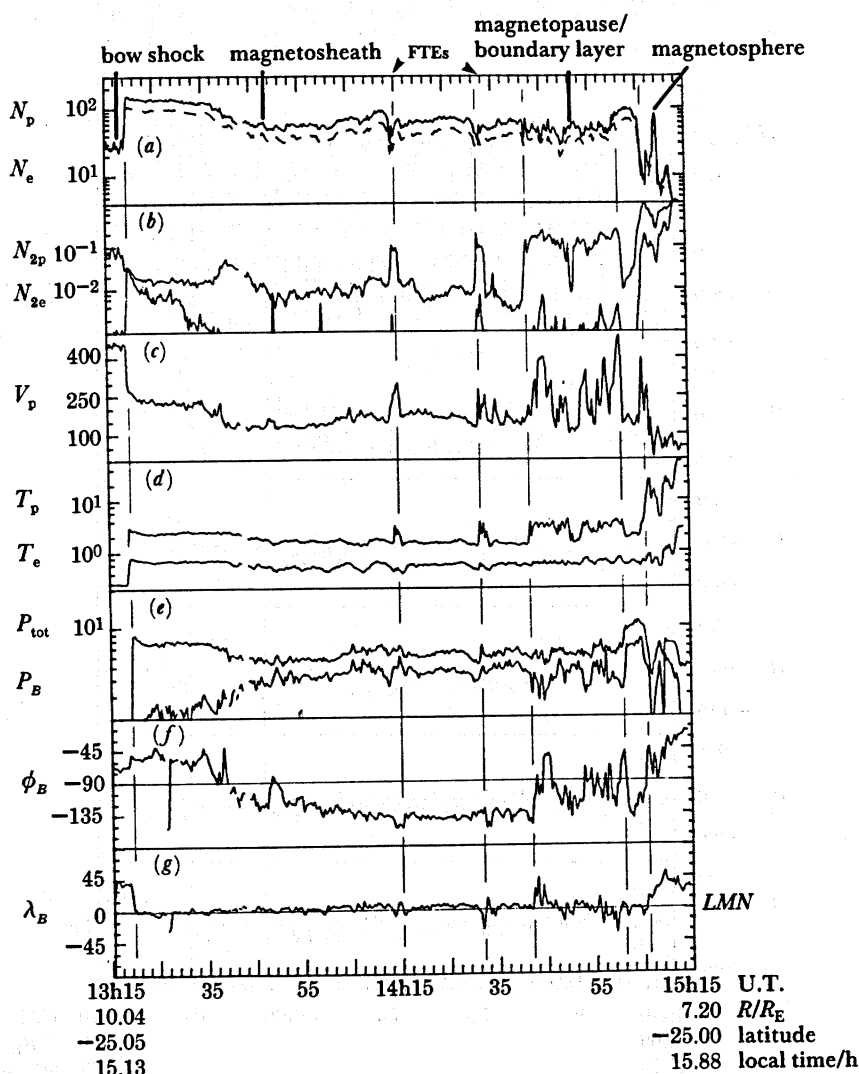


FIGURE 4. Two-hour data overview of the inbound pass on 4 September 1984 starting from the bow shock (to the left) to the long magnetopause/boundary layer crossing (to the right). (a) Proton and electron densities (cm^{-3}); (b) partial densities (cm^{-3}) of protons ($> 9 \text{ keV}$) and electrons ($> 1.8 \text{ keV}$); (c) proton bulk speed (km s^{-1}); (d) proton and electron temperatures (10^6 K); (e) magnetic field and total pressure (nPa); (f) field azimuth and (g) elevation angles (deg) in LMN coordinates. (After Paschmann *et al.* (1986).)

latitudes, mid-afternoon local time. The top panel shows the proton and electron densities: low, sunwards of the bow shock position on the left, high in the magnetosheath, dropouts during the FTES and dropping to low magnetospheric values once inside the terrestrial field. An azimuth angle ϕ_B less than -90° indicates a sheath field pointing south.

Figure 5 is a close-up view of the magnetopause encounter showing the field and flow components in the bottom six panels and the energetic proton heat flux along the magnetic field in the second panel. The coordinates x , y and z correspond to the boundary normal coordinates L , M and N respectively. We note in particular the two shaded panels where large, anti-correlated variations in the L -components of the field and flow are observed. This is expected for a rotational discontinuity when the velocity and field components normal to the

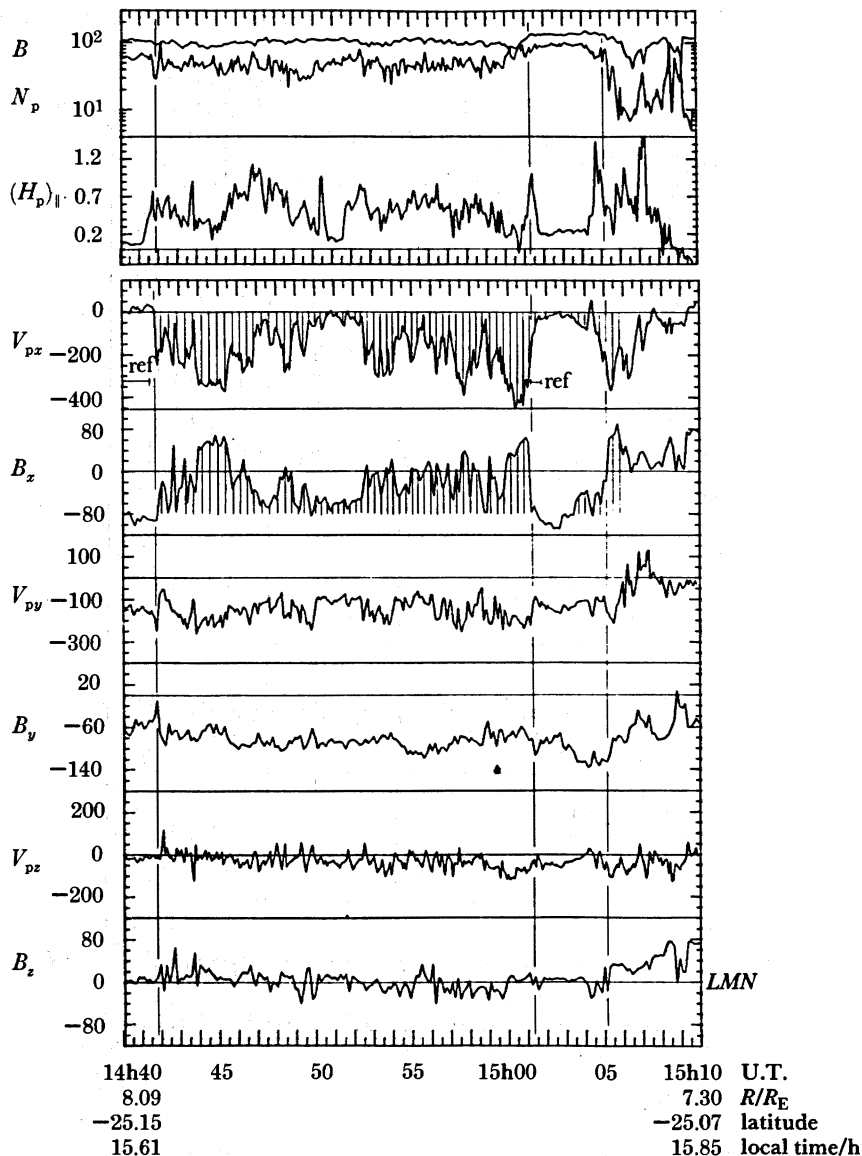


FIGURE 5. The passage of AMPTE-IRM through the magnetopause on 4 September 1984. The coordinates x , y , z correspond to the boundary normal coordinates L , M , N respectively. More details are given in the text. (After Paschmann *et al.* (1986).)

magnetopause have opposite signs. As we assume inflow, i.e. negative V_N , this implies that the normal field component, B_N , is positive. This in turn means that the magnetic field connects to the Southern Hemisphere. The inferred crossing south of the reconnection line is confirmed by the sign of the computed heat fluxes along the field (second panel) which, being positive, indicates magnetospheric ions streaming out parallel to the field.

The results of applying the stress balance and energy balance tests mentioned earlier are shown in figure 6. The first panel is a test of tangential flow magnitudes with respect to the theoretical value. The observed changes in flow speeds between points in the magnetopause/boundary layer and a sheath reference interval divided by the theoretically predicted differences are plotted in (a). This is quite good in general, but there are occasional discrepancies. Graph (b) tests the direction of these flow vectors, $\delta_{0,t}$ being the angle in the magnetopause plane between theoretical and measured velocity difference vectors. A value of 180° for $\delta_{0,t}$, as here, implies a positive B_N . The agreement is good. Parameter Σ_E in (c) gives the sum of the energy terms normalized to a reference value in the sheath. Perfect agreement would give 1. This is approximately what is obtained.

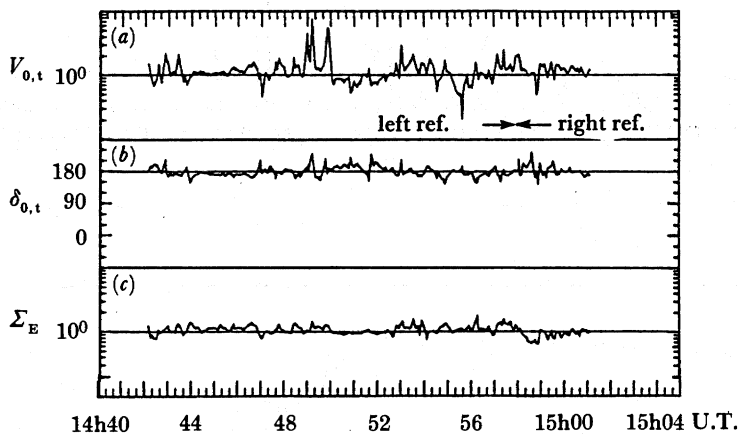


FIGURE 6. The results of the stress balance and energy balance tests for the high-speed flow encountered on 4 September 1984. (a) Magnitude of the measured flow difference vectors (magnetopause/boundary layer against sheath reference interval) relative to the theoretically predicted ones. (b) Angles in the LM -plane which the observed difference vectors make with the theoretical vectors. (c) Sum of the measured energy terms normalized to the magnetosheath reference value. (After Paschmann *et al.* (1986).)

3.2. Flux transfer events: AMPTE observations

Turning now to *AMPTE* observations of FTES, we shall briefly discuss some results from three recent works. The first, by LaBelle *et al.* (1987), surveyed wave emissions in magnetospheric FTES observed by *AMPTE-IRM* during the fall of 1984. Four distinctive types of wave activity were found, three of which might be identified with waves studied earlier by Anderson *et al.* (1982) in conjunction with magnetosheath FTES using *ISEE* data. These are (i) an intensification of electromagnetic emission in a frequency range from a few hertz to a few hundred hertz, and in which most of the power resides; (ii) broadband, electrostatic, spike-like emissions in a medium frequency range (200 Hz to *ca.* 2.5 kHz) and (iii) large-amplitude (at most 10 nT) magnetic field fluctuations of frequency below the ion gyrofrequency. Generally, all these emissions are confined to the 'interior' of the FTE structure. An interesting new feature

reported is the electron wave bursts near the electron plasma frequency. In contradistinction to the other emissions, these occur at the edges of the FTE signature. Furthermore, they are extremely common.

To illustrate this feature, figure 7 *b, c* shows high-resolution field data for an FTE observed on 28 October 1984. (*a*) is a frequency against time plot with only the high (9–99 kHz) frequencies shown. The power spectral density is displayed on a grey scale. The solid line in (*a*) is a trace of the electron plasma frequency. The electron wave emissions are shown arrowed. Another type of wave activity (type (iii) above) can be seen in the low-frequency magnetic oscillations of the B_N component in (*c*). Finally, we note the peculiar field strength profile shown in (*b*). This represents a detail of the field first observed clearly with *AMPTE* high-resolution data.

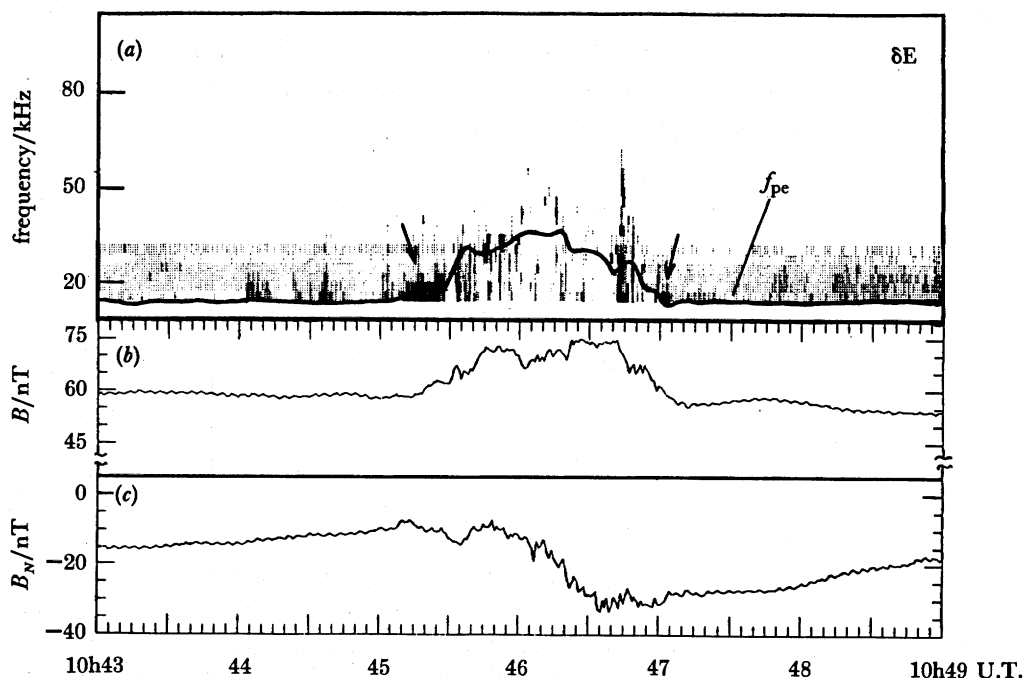


FIGURE 7. *AMPTE-IRM* data relating to an FTE on 28 October 1984. (*a*) High-frequency emissions are shown with the power plotted by using a grey scale. (*b*) Field strength profile. (*c*) Variation of the field component normal to the magnetopause. Note in (*a*) the electron wave bursts, which are arrowed, occurring at the edges of the FTE near the electron plasma frequency (solid trace). (After LaBelle *et al.* (1987).)

Interestingly enough, at about the same time that LaBelle *et al.* were recording their observations, Rijnbeek *et al.* (1987), our second work on FTEs) were studying the same FTE from a different viewpoint. They undertook to separate neatly *in the data* (as opposed to ‘in the model of figure 3’) the region of field-line draping, as we explained in the cartoon (figure 3) earlier, from that of the internal, twisted field-line region. This they were able to do. In the course of the investigation, however, they noted that the ‘periphery’ of the postulated flux tube was by no means sharp. Instead, it turned out to be a region of large spatial extent (some 10 ion gyroradii thick, *ca.* $1 R_E$). This region had distinct properties. The plasma density exhibited a gradient from low magnetospheric to high sheath-like values and there were enhanced fluxes of medium energetic (*ca.* 200 eV) electrons. There was also a peculiar magnetic field behaviour in the plane tangent to the magnetopause. Having deflected one way in the draped field-line

region, it reversed its sense of rotation as it crossed this region. This reverse field tilt indicates that large currents are flowing along the flanks of the reconnected flux tube. For these reasons they proposed stratifying the FTE signature into three regions rather than the two required by the Russell–Elphic model. We illustrate this study by three figures.

Figure 8 shows 6 min of half-second resolution magnetic field data. The data are plotted in boundary normal coordinates. The departure of B_N from ambient values gives the duration of the FTE as 5.4 min. The vertical lines indicate times when the region boundaries were encountered. From the order in which they are crossed, one infers that they are nested.

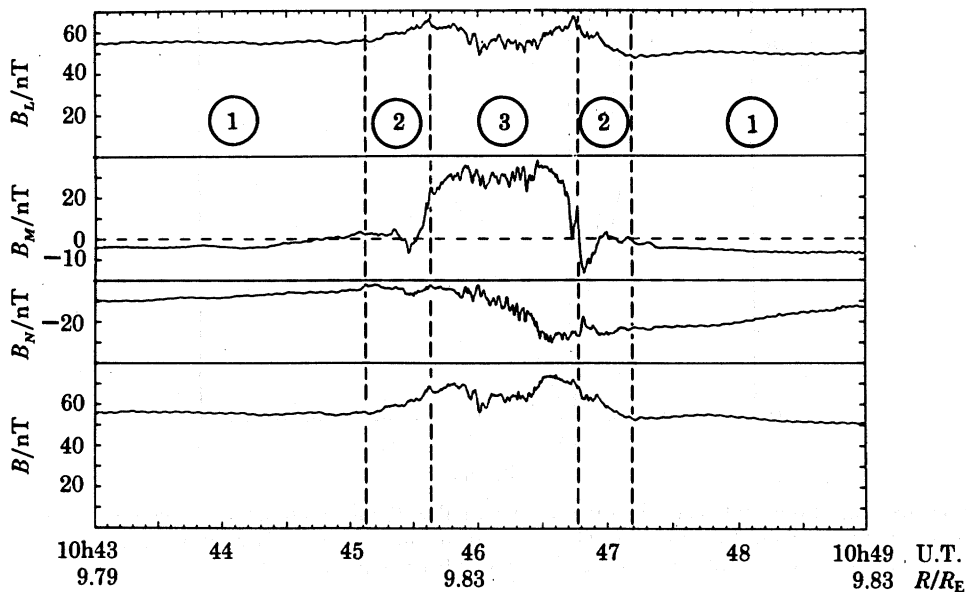


FIGURE 8. 6 min of AMPTE-UKS half-second resolution field data for the same FTE as in figure 7. The coordinates are boundary normal. The vertical guidelines separate regions where different properties were seen in the data. Local time was 08h34 and the latitude was 2° . (After Rijnbeek *et al.* (1987).)

Figure 9 shows the field tilts as we go from one region to the next. We chose to show the ‘exit leg’, from 10h46 to 10h49 U.T. The vector, OZ' in the $B_L B_M$ -plane gives the field orientation reached in the internal twisted region. The field vector first fluctuates about this mean orientation. Then it rotates anticlockwise by *ca.* 30° , and overshoots the ambient magnetosphere orientation, represented by the vector OX' . This is region 3. There follows a clockwise rotation, comprising the reverse tilt in region 2 mentioned earlier. Finally, the sense of tilt is again reversed and the remaining rotation results from the draped field.

Figure 10 shows the electron intensities at three different energies. The top trace – for 12 eV electrons, an energy typical of the sheath – reaches a maximum at the centre. The bottom trace indicates complete disappearance of 980 eV electrons, typical of the magnetosphere, at the centre. The middle trace, corresponding to 205 eV electrons, reaches maximum values in the newly discovered region. Vertical lines coincide with the changes in the sense of field deflection of figure 9.

The report of Farrugia *et al.* on FTE structure (1988, our final AMPTE FTE example) presented a study of seven magnetospheric FTEs. The observations spanned a 40° latitude range from early dawn to mid-afternoon local times. They confirmed the layering thesis of Rijnbeek

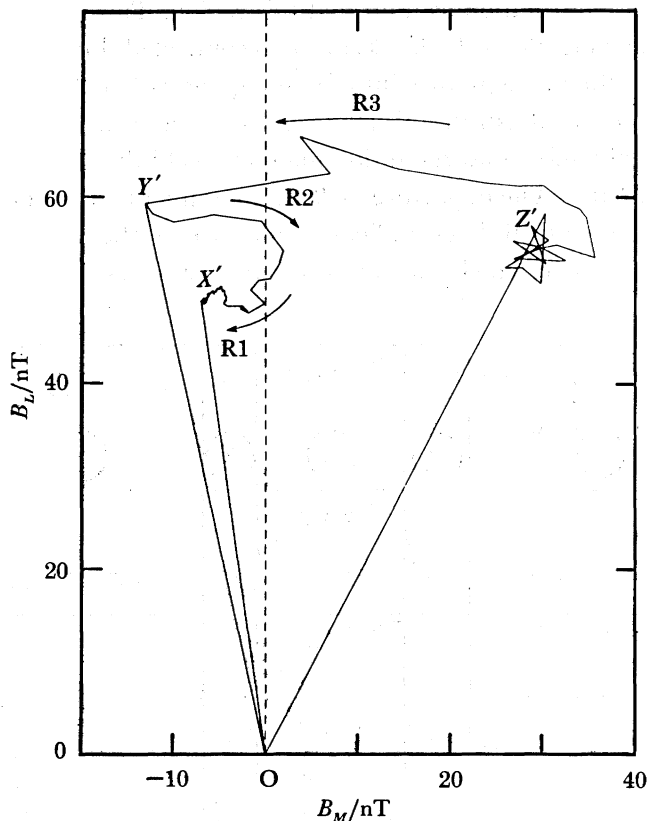


FIGURE 9. Deflections of the field vector in a plane tangential to the magnetopause for the later part of the FTE on 28 October 1984 (10h46–10h49 U.T.). The ambient magnetosphere field orientation is given by the vector OX' . Note the reverse field tilt in region 2. (After Rijnbeek *et al.* (1987).)

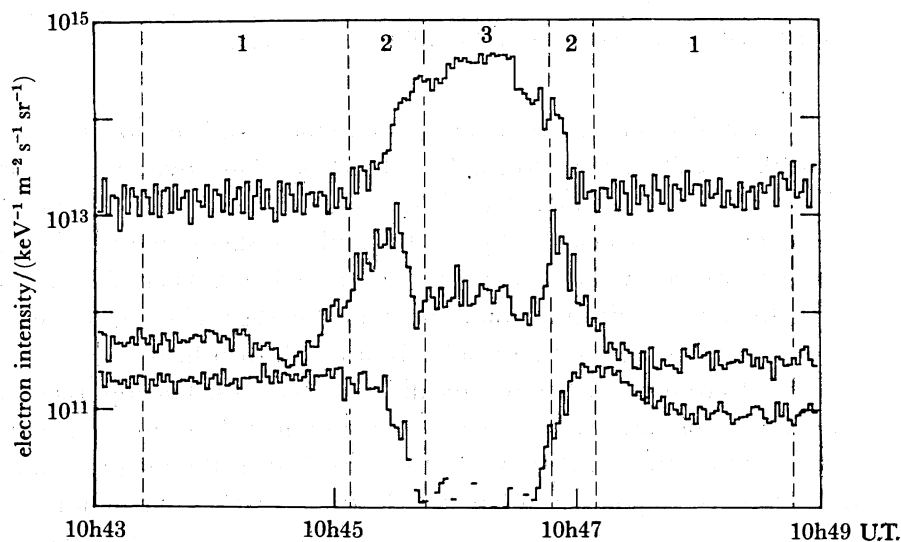


FIGURE 10. Electron intensity at three different energies through the same FTE as in the previous three plots (orbit 40, day 84–302). The top trace refers to 12 eV electrons; the middle to 205 eV electrons; the bottom one to 980 eV electrons. Note the order-of-magnitude increases in the medium energetic electrons in region 2. (After Rijnbeek *et al.* (1987).)

et al. where each FTE region had distinct properties in the field, plasma properties and population characteristics, and wave emissions. To be sure, the events did not show exactly the same behaviour but they had strong similarities. Much activity was found in region 2 of Rijnbeek *et al.* For instance, the hot electrons in this layer were found to be counterstreaming, an interesting discovery. The emissions near the electron plasma frequency which were seen by LaBelle *et al.* (1987) occur precisely in this region and such electron beams are a likely source. In this region there was also evidence of heating of ions, and flow enhancements over and above the flow increases seen in the rest of the FTE were often observed.

A likely explanation for these observations is continued reconnection even as the observations are made. If this is the case, the instances of dramatic flow shears associated with some high-speed flows in region 2 seen by Farrugia *et al.* (see their figure 11) may be explicable in terms of a moving reconnection line.

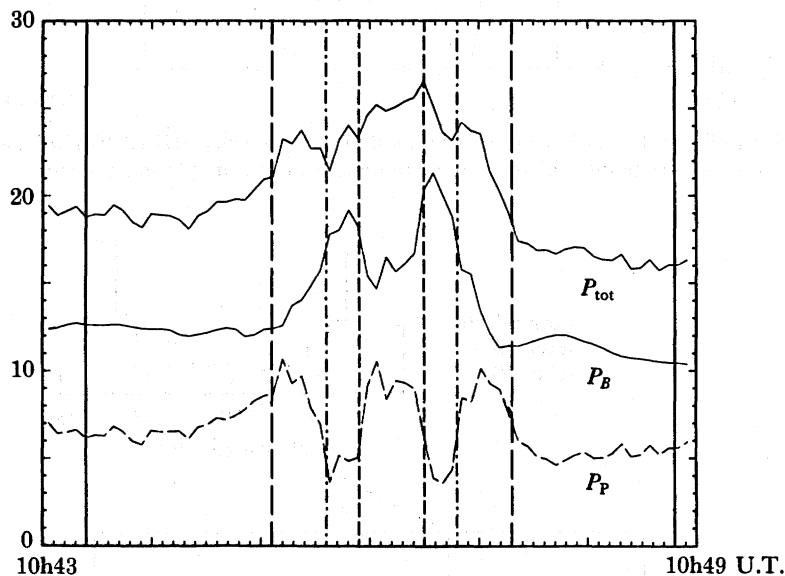


FIGURE 11. The variations of the plasma pressure (P_p), the magnetic field pressure (P_B) and the total pressure (P_{tot}) during the same FTE. The antiphase relation of P_p and P_B is clear. (After Farrugia *et al.* (1988).)

Interesting new results emerged on the interplay between the field and plasma pressures. Past work showed the total pressure inside FTEs to exceed ambient values and, indeed, tension of the curved and draped field lines was invoked to contain this pressure (Paschmann *et al.* 1982). Here it was found that the field and plasma pressure can vary a great deal individually but they counterbalance each other, maintaining the total pressure excess. This strictly anticorrelated behaviour was found even in those extreme circumstances when the field strength dropped to almost zero.

We illustrate some results of this work with three figures. Figure 11 shows the variation of the plasma and field pressures, again for the 28 October event. The antiphase behaviour is evident, leading to large variations in the plasma beta (the ratio of the plasma pressure to the magnetic energy density). The vertical guidelines show the regions where, on other grounds, region 3 of Rijnbeek *et al.* has been further subdivided into two regions, R3 and R4.

Similar information is shown for an event encountered on 6 December 1984 (figure 12). At

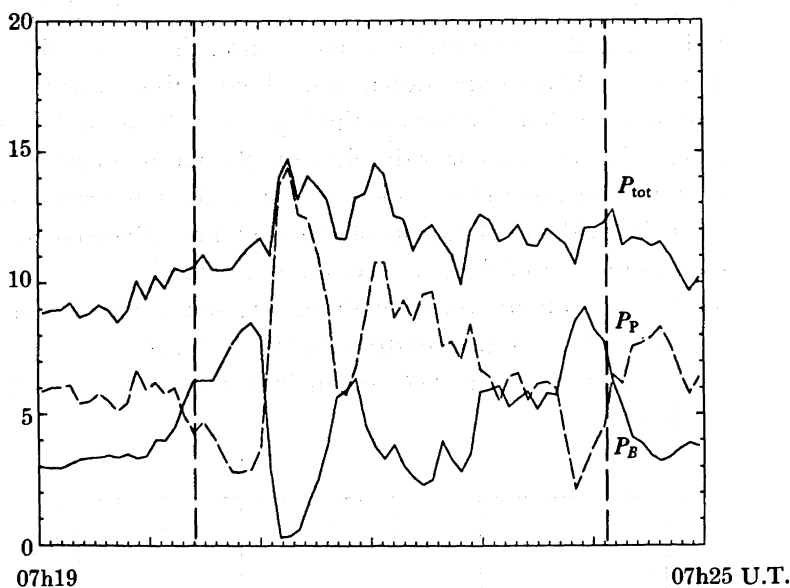


FIGURE 12. Similar to figure 11 but for an FTE seen on 6 December 1984 (07h19–07h25 U.T.). Note the dropout of field pressure at one point which is compensated by a rise in plasma pressure. (After Farrugia *et al.* (1988).)

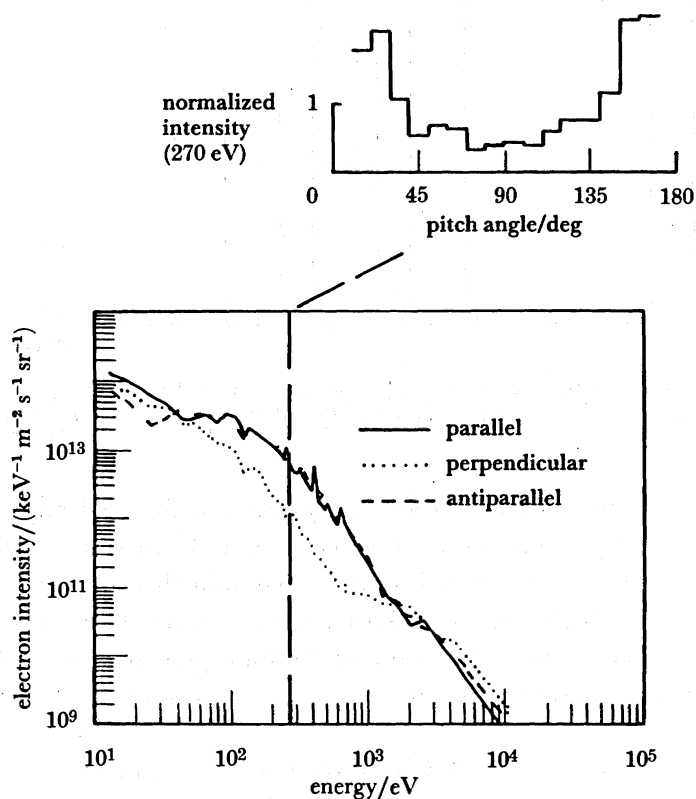


FIGURE 13. Electron intensity against energy for the 28 October 1984 FTE discussed earlier. The increase in intensity of medium energetic electrons is mainly as a result of counterstreaming electron beams. The inset shows a pitch angle distribution of normalized intensities for 270 eV electrons. (After Farrugia *et al.* (1988).)

one point the field decreases almost to zero but the dropout in field pressure is compensated by a rise in the plasma pressure. We recall that in the past it was often thought that the field strength in FTEs shows a simple enhancement maximizing at the centre. *AMPTE* teaches us otherwise.

Finally, we show the counterstreaming electrons, again from the October 28 event (figure 13, 10h45:20–10h45:40). The electron intensity is shown plotted against energy for three different directions: parallel, perpendicular and antiparallel to the field. It is clear that the increase in intensity is associated with field-aligned electrons. This is shown explicitly with the full pitch angle distribution for 270 eV electrons in the inset.

4. RECENT ADVANCES IN THEORY AND DATA INTERPRETATION RELATING TO RECONNECTION

4.1. *Time-independent reconnection*

In the last part of this article we discuss recent theoretical progress and its impact on data interpretation. We start with time-independent reconnection.

Most quantitative analyses of steady reconnection at the terrestrial magnetopause start with Petschek's (1964) fluid model for the reconnection process. Petschek postulated standing MHD (magnetohydrodynamic) waves as a means by which magnetic energy can be more effectively converted into plasma energy. Figure 14 illustrates Petschek's scenario. In the centre we have

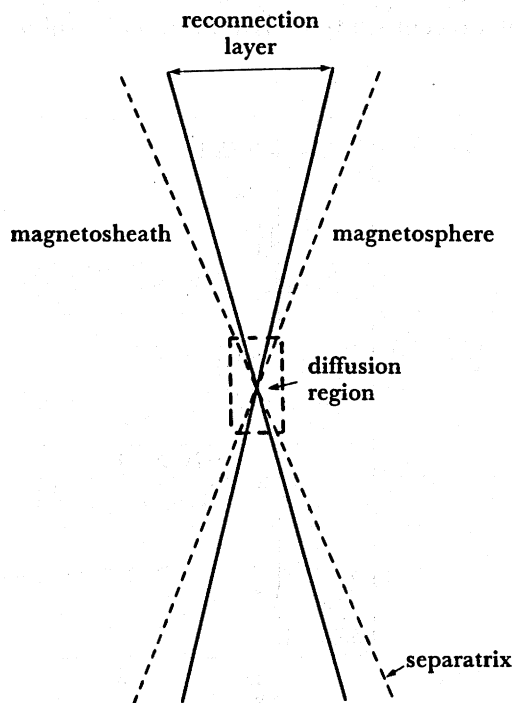


FIGURE 14. Petschek's reconnection configuration for reconnection at the Earth's magnetopause. Standing MHD waves make up the reconnection layer. This layer is susceptible to analysis by ideal MHD. A much smaller diffusion layer, where an ideal MHD description is not appropriate, surrounds the reconnection line at the centre. The inflow magnetosheath and magnetospheric regions in a plane tangential to the magnetopause are also shown.

a reconnection line surrounded by a small diffusion region. Either side we have a layer of MHD waves propagating away from the diffusion region. This is the reconnection layer. It allows the parameter values in the magnetosheath and magnetosphere adjacent to the layer, the inflow regions, to be matched.

Petschek analysed the symmetric situation where the field and plasma in the inflow region had identical parameters, the fields were strictly antiparallel and the tangential velocities in the inflow region were zero. His reconnection layer then consisted of two slow switch-off shocks. Subsequently, Levy *et al.* (1964) discussed qualitatively the effect of an extreme asymmetry in the density. The sheath Alfvén wave which appears in the presence of any asymmetry to rotate the fields has become the cornerstone of analyses of magnetopause high-speed flow data, as we saw earlier.

None of these models are strictly applicable to reconnection at the dayside magnetopause. However, recent work by Heyn *et al.* (1988) has elaborated a detailed structure of the reconnection layer for the general case of unequal plasma densities, arbitrary magnetic fields and plasma velocities. A study of the application of this theory to parameter régimes typical of the terrestrial magnetopause has very recently been carried out by Biernat *et al.* (1989). It can now be applied to the AMPTE data-set, for instance to the 4 September 1984 HSRF encounter discussed earlier. Moreover, the Petschek reconnection model can now be tested for a wide range of conditions. We mention in this context the Gosling *et al.* (1982) discovery of high-speed flows at a magnetopause crossing under highly unusual conditions.

Rather than examine the details of the theory, we shall compare its predictions with the observations on the first and possibly best-known reconnection example to data: 8 September 1978. This is the subject of a recent study by Rijnbeek *et al.* (1989). Figure 15 shows magnetic

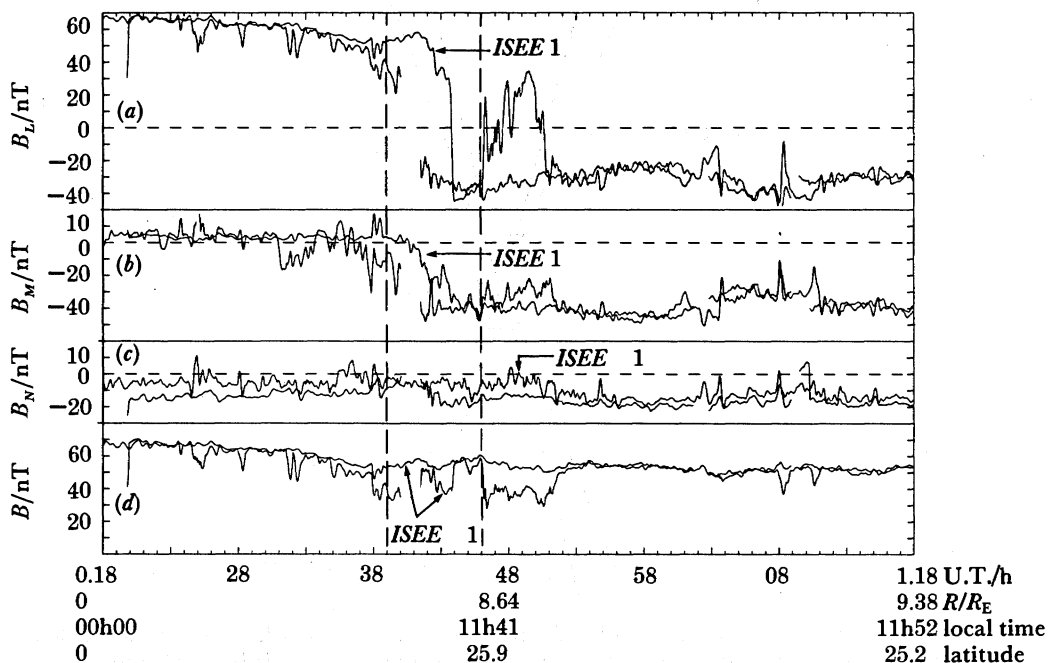


FIGURE 15. ISEE 1 magnetic field data for an outbound crossing of the magnetopause on 8 September 1978. We study ISEE 1 data (dark trace) during the interval shown within vertical guidelines. (After Rijnbeek *et al.* (1989).)

field data for the magnetopause crossing in question. We study *ISEE 1* data (dark trace). During the seven-minute interval shown within vertical guidelines, high-speed flows were seen. Within this interval there is the reconnection layer, which is identified from the rotation of the field from a magnetosphere to a magnetosheath orientation. Note the field drop in (d) , as well as the resemblance of the data to figure 2.

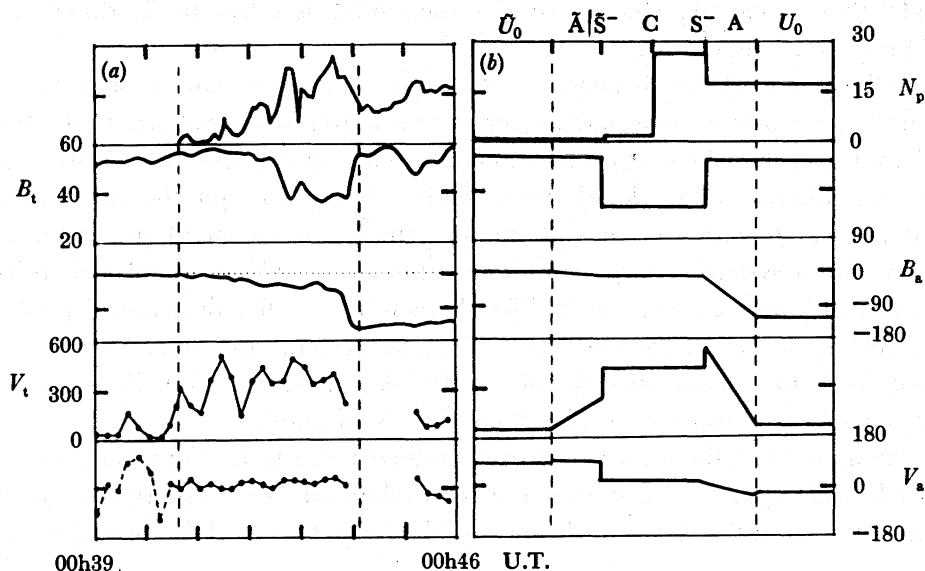


FIGURE 16. Theoretical predictions (Heyn *et al.* 1988*a*) of the reconnection layer for the inflow parameters on 8 September 1978 (b) compared with field and plasma observations during *ISEE 1*'s outbound passage through the reconnection layer on that day (a) . The reconnection layer is shown within vertical guidelines. (b) A, S, C correspond to Alfvén wave, slow shock and contact discontinuity respectively. Quantities with and without a tilde refer to magnetospheric and magnetosheath quantities respectively. U (\tilde{U}) stands for the magnetospheric (magnetosheath) set of inflow parameters. Other quantities are explained in the text. (After Rijnbeek *et al.* (1989).)

We then input the inflow parameters, corrected for the presence of heavy ions (which have been observed and reported by Sonnerup *et al.* (1981) and by Peterson *et al.* (1982). Figure 16*b* shows the theoretical predictions. To the left is the magnetosphere; to the right, the sheath. The whereabouts of the reconnection layer is shown between vertical guidelines. The reconnection layer structure which results, shown at the top of the figure, has two Alfvén waves, enclosing two slow shocks, with a contact discontinuity in between. The N_p panel gives the variation in the ion density; the B_t panel shows the variation in the tangential field strength through the layer; B_s is the field angle in the tangential plane; V_t is the predicted magnitude of the high-speed flows and V_s , the angle of the velocity vector in the LM -plane. Comparison with data shown in the same format in figure 16*a* immediately shows that there are many points of agreement: a field strength decrease is predicted and observed; the variations in the field angle are similar; plasma flow enhancements of the right magnitude are predicted, and there is an increase in the plasma density, N_p , as predicted. The discrepancies centre around (a) a blurred contact discontinuity (presumably due to leakage of dense sheath plasma); (b) a field rotation overlapping the field strength decrease (possibly due to coupling of the sheath Alfvén wave with the slow shock). This latter might be a reflection of non-uniformities in the inflow region, whereas the theory of Heyn *et al.* (1988) assumes uniformity there. None the less, the points of agreement are quite striking.

4.2. Time-dependent reconnection

Our final topic is time-dependent reconnection. The most recent work on this subject is by Southwood *et al.* (1988) who invoke changes in the reconnection rate and are thus able to account for many of the newer observations on FRES which we mentioned earlier. The geometry of the model they proposed, which is three dimensional, is substantially different from the Russell–Elphic model (figure 3).

Earlier, following work by Semenov *et al.* (1984) and Pudovkin & Semenov (1985), a rigorous mathematical treatment under symmetric conditions was elaborated by Biernat *et al.* (1987). Biernat *et al.* show how a perturbation of the current strength at a certain region of the magnetopause, initially a tangential discontinuity, leads, through the small normal field component associated with the current inhomogeneity, to the break-up of the tangential discontinuity into a system of large-amplitude MHD waves. These bound a shell-like region across which field lines are reconnected. The shape of this shell is determined predominantly by the time history of the electric field, $E_r(t)$, along the reconnection line. An increase in $E_r(t)$, for example, leads to a spatial broadening of the reconnection region. Reconnection ceases when $E_r(t)$ goes to zero and it is steady when $E_r(t)$ is constant.

A data example using these ideas has been studied recently by Farrugia *et al.* (1989; see also Rijnbeek *et al.* 1984*b*). Because its aim is to relate all three signatures of reconnection which we mentioned at the start, this brings us full circle. This work is the subject of our next discussion.

Figure 17 presents low-resolution magnetic field data for an outbound magnetopause

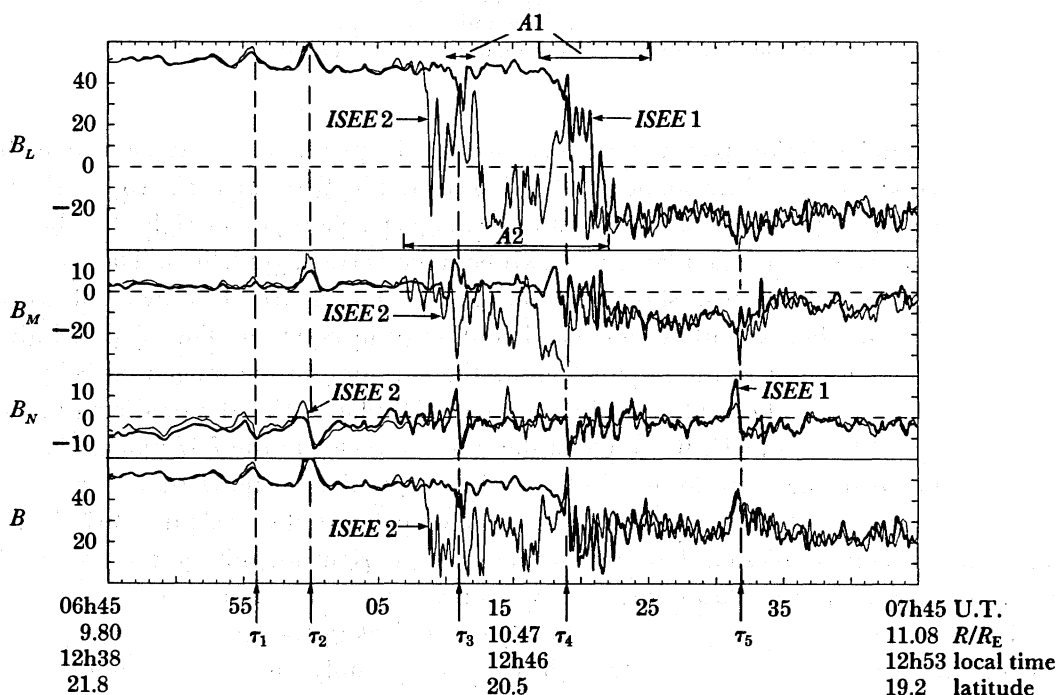


FIGURE 17. ISEE 1 and 2 magnetic field data for an outbound crossing of the magnetopause on 3 September 1978. A1, A2 refer to intervals where HSFs were seen on ISEE 1, ISEE 2, respectively. The symbols τ_1 – τ_5 are introduced for ease of reference. (After Farrugia *et al.* (1989).)

crossing on 3 September 1978. *ISEE 2* leads *ISEE 1* by *ca.* 1000 km almost exclusively along the normal direction to the magnetopause. *A1* and *A2* bracket regions where high-speed flows were seen (Sonnerup *et al.* 1981).

The spacecraft move outwards towards the magnetopause and at τ_1 , and 5 min later at τ_2 , an FTE is observed by both spacecraft. The spacecraft closest to the magnetopause (*ISEE 2* at this time) sees the stronger signature not only in the field data, but also in the plasma. (We mention in passing that on *ISEE 1* a plasma signature is absent altogether during the observation marked τ_1 in figure 17 so that the field perturbations we see there are caused by draping.) When *ISEE 2* exits the magnetosphere, we see a concertina-like structure in B_L . These are the B_L spikes. If we look carefully, there are ‘sympathetic’ variations in the B_L component on *ISEE 1*, further earthwards. Higher-resolution data confirm that these are in strict one-to-one correspondence with the B_L spikes seen on *ISEE 2*. *ISEE 1* is observing perturbations of the magnetospheric inflow region caused by the reconnection process even as *ISEE 2* is monitoring perturbations of the outflow region itself. There also occur field strength drop-outs during the observations of B_L spikes (figure 17). There is plenty of B_N activity with some coincident signatures. In particular, we mention the event τ_3 , another simultaneous observation of an FTE by both spacecraft. This is not quite an instance of a two-régime FTE observation of the type studied elsewhere (Farrugia *et al.* 1987*b*), where two spacecraft on opposite sides of the magnetopause see the same FTE simultaneously. During τ_3 one spacecraft (*ISEE 1*) remains in the magnetosphere while the other is crossing the reconnection layer. During this observation, the B_M component of *ISEE 1* goes one way while that of *ISEE 2* goes the other way. A few minutes later *ISEE 1* exits, B_L spikes appear and there is also a resumption of such activity at *ISEE 2*, 1000 km further sunwards. Our considerations end at τ_5 , another simultaneous FTE observation, this time in the sheath.

Figure 18 shows how we postulate the reconnection layer might be shaped when a time-dependent reconnection electric field is present. The outflow angle, γ , measuring the rate at which flux is reconnected, varies and these variations give rise to the ‘corrugations’ shown in the figure. Some are large, some are small. The disturbances in the reconnection layer’s boundary are drawn ‘out of phase’ with each other and should be carefully distinguished from surface waves arising from the Kelvin–Helmholtz instability.

The plasma is being accelerated along L . On this picture, the larger corrugations correspond to FTEs with well-defined B_N signatures. To illustrate this, we have drawn the trajectories of the spacecraft during the FTE observation τ_3 . Note that the continuity of B_N is guaranteed by the field twist. Thus, in τ_3 for example, *ISEE 1* on the right sees a field increase into the plane of the paper (i.e. along $+M$) and *ISEE 2* out of the paper. As suggested by the diagram, this twist exists throughout the reconnection layer and is probably the result of the distributions of currents which are caused by an explicitly time-varying reconnection electric field.

Any partial entry into the reconnection layer from the sheath side gives rise to substantial changes in B_L as the fields in the sheath and in the reconnection layer have very different L -components. However, the accompanying changes in the normal field component, B_N , need not be large or smooth because the corrugations may have a small curvature and the fluctuations in the reconnection rate may be erratic. This is the explanation for the B_L spikes.

The reconnection layer’s outflow angle γ may open and close. Data not shown here (see Farrugia *et al.* 1989) indicate that this might have been the case particularly for the crossing by the first spacecraft, which appears in many respects much more ‘bursty’ than the other. In

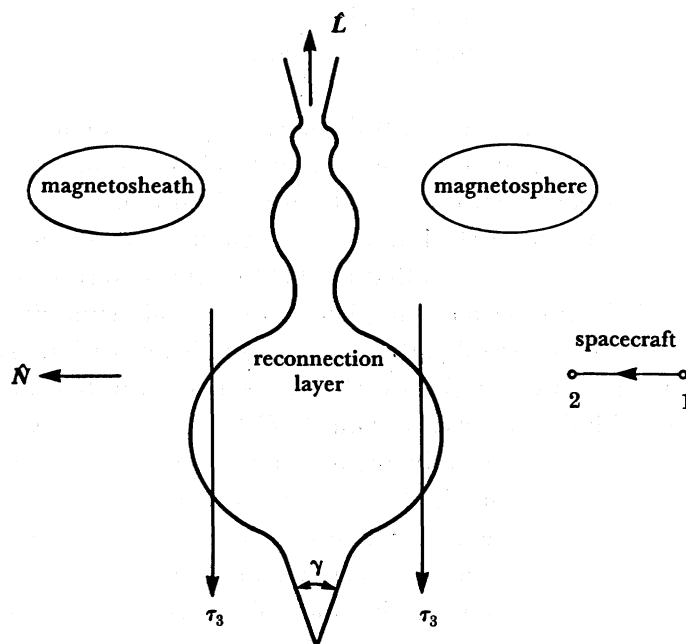


FIGURE 18. A postulated schematic of the reconnection layer in the LN -plane for a time-dependent Petschek reconnection scenario. The outflow opening angle γ varies as the reconnection rate changes, giving rise to a 'corrugated' boundary as shown. The arrows indicate the direction of motion of *ISEE 1* (to the right) and *ISEE 2* (to the left) relative to the reconnection layer during the simultaneous observation of an FTE by the spacecraft pair in the event marked τ_3 in the previous figure. (After Farrugia *et al.* (1989).)

that case the diffusion layer collapses and is rebuilt. The debris is swept with the flow. In short, we are speculating that the field strength drops might be a signature of the diffusion region.

Can the observations on 3 September 1978 be accounted for by surface waves on a boundary which has become Kelvin–Helmholtz unstable? This is unlikely. Firstly, the boundary on this day satisfies the condition for Kelvin–Helmholtz stability of two incompressible plasmas separated by a tangential discontinuity (Landau & Lifshitz 1960; Biernat *et al.* 1989). Secondly, surface waves would fail to explain the repeated observations of pairs of similar features occurring simultaneously on both spacecraft. To give an example, just before the event marked τ_4 (figure 16), *ISEE 2* was in the sheath and *ISEE 1* was in the magnetosphere, i.e. they were both outside the reconnection layer. On the surface wave picture, one would intuitively expect that the passage of such a wave would either leave both the spacecraft where they are or would cause one of them to enter the layer and one to remain outside. However, figure 16 shows what in fact happens during τ_4 ; both spacecraft enter the layer simultaneously.

5. CONCLUDING REMARKS

It is evident that the improved instrumentation on the *AMPTE* mission has furnished a wealth of detailed observations in the field of solar-wind–magnetosphere coupling. Further insights into the reconnection process, both steady and unsteady, at the dayside magnetopause have been provided by recent theoretical work. This has given fresh stimulus to the interpretation of data. In turn, some aspects of present data analysis are in some sense an

extrapolation of existing theories and thus they still require rigorous theoretical validation. As we are far from exhausting the possibilities of the *AMPTE* data-set, it is fair to expect this cross-fertilization of theory and observation to intensify.

It is my pleasure to thank colleagues Helfried Biernat, Martin Heyn and Richard Rijnbeek for helpful discussions of the above material. I also thank them for their hospitality during my visit to the Institut für Weltraumforschung in Graz, Austria, on a European Science Exchange Programme grant sponsored by the Royal Society. G. Paschmann and R. A. Treumann kindly supplied the plots for figures 4–7. I also thank D. J. Southwood and S. W. H. Cowley for their support.

REFERENCES

- Anderson, R. R., Harvey, C. C., Hoppe, M. M., Tsurutani, B. T., Eastman, T. E. & Etcheto, J. 1982 Plasma waves near the magnetopause. *J. geophys. Res.* **87**, 2087.
- Berchem, J. & Russell, C. T. 1984 Flux transfer events on the dayside magnetopause: Spatial distribution and controlling factors. *J. geophys. Res.* **89**, 6689.
- Biernat, H. K., Heyn, M. F., Rijnbeek, R. P., Semenov, V. S. & Farrugia, C. J. 1989 The structure of reconnection layers: application to the Earth's magnetopause. (In the press.)
- Biernat, H. K., Heyn, M. F. & Semenov, V. S. 1987 Unsteady Petschek reconnection. *J. geophys. Res.* **92**, 3392.
- Cowley, S. W. H. 1982 The causes of convection in the Earth's magnetosphere – a review of developments during the IMS. *Rev. Geophys. Space Phys.* **20**, 531.
- Dungey, J. W. 1961 Interplanetary magnetic field and the auroral zones. *Phys. Rev. Lett.* **6**, 47–48.
- Farrugia, C. J., Rijnbeek, R. P., Saunders, M. A., Southwood, D. J., Smith, M. F., Rodgers, D. J., Christiansen, P. J., Chaloner, C. P., Woolliscroft, L. J. C. & Hall, D. S. 1988 A multi-instrument study of flux transfer event structure. *J. geophys. Res.* **93**, 14465.
- Farrugia, C. J., Rijnbeek, R. P., Biernat, H. K., Heyn, M. F., Cowley, S. W. H., Southwood, D. J., Semenov, V. S., Haerendel, G., Paschmann, G. & Russell, C. T. 1989 Flux transfer events and their relationship to other reconnection-associated signatures. (In the press.)
- Farrugia, C. J., Elphic, R. C., Southwood, D. J. & Cowley, S. W. H. 1987a Field and flow perturbations outside the reconnected field line region in flux transfer events: theory. *Planet. Space Sci.* **35**, 227.
- Farrugia, C. J., Southwood, D. J., Cowley, S. W. H., Rijnbeek, R. P. & Daly, P. W. 1987b Two-regime flux transfer events. *Planet. Space Sci.* **35**, 737.
- Gosling, J. T., Asbridge, J. R., Bame, S. J., Feldman, W. C., Paschmann, G., Scokopke, N. & Russell, C. T. 1982 Evidence for quasi-stationary reconnection at the dayside magnetopause. *J. geophys. Res.*, **87**, 2147.
- Heyn, M. F., Biernat, H. K., Rijnbeek, R. P. & Semenov, V. S. 1988 The structure of reconnection layers. *J. Plasma Phys.* **40**, 235.
- Hudson, P. D. 1970 Discontinuities in an anisotropic plasma and their identification in the solar wind. *Planet. Space Sci.* **18**, 1611.
- Johnstone, A. D., Rodgers, D. J., Coates, A. J., Smith, M. F. & Southwood, D. J. 1986 Ion acceleration during steady-state reconnection at the dayside magnetopause. In *Ion Acceleration in the Magnetosphere and Ionosphere*. *Geophys. Monograph Ser.* (ed. T. Chang), vol. 38, p. 136. Washington, D.C.
- LaBelle, J., Treumann, R. A., Haerendel, G., Bauer, O. H., Paschmann, G., Baumjohann, W., Lühr, H., Anderson, R. R., Koons, H. C. & Holzworth, R. H. 1987 *AMPTE-IRM* observations of waves associated with flux transfer events in the magnetosphere. *J. geophys. Res.* **92**, 5827.
- Landau, L. D. & Lifshitz, E. M. 1960 *Electrodynamics of continuous media*. New York: Pergamon Press.
- Levy, R. H., Petschek, H. G. & Siscoe, G. L. 1964 Aerodynamic aspects of the magnetospheric flow. *AIAA JI* **2**, 2065.
- Paschmann, G., Haerendel, G., Papamastorakis, I., Scokopke, N., Bame, S. J., Gosling, J. T. & Russell, C. T. 1982 Plasma and magnetic field characteristics of magnetic flux transfer events. *J. geophys. Res.* **87**, 2159.
- Paschmann, G., Papamastorakis, I., Baumjohann, W., Scokopke, N., Carlson, C. W., Sonnerup, B. U. O. & Lühr, H. 1986 The magnetopause for large magnetic shear: *AMPTE/IRM* observations. *J. geophys. Res.* **19**, 11099.
- Paschmann, G., Papamastorakis, I., Scokopke, N., Sonnerup, B. U. O., Bame, S. J. & Russell, C. T. 1985 *ISEE* observations of the magnetopause: reconnection and the energy balance. *J. geophys. Res.* **90**, 12111.
- Paschmann, G., Sonnerup, B. U. O., Papamastorakis, I., Scokopke, N., Haerendel, G., Bame, S. J., Asbridge, J. R., Gosling, J. T., Russell, C. T. & Elphic, R. C. 1979 Plasma acceleration at the earth's magnetopause: evidence for reconnection. *Nature, Lond.* **282**, 243.

- Peterson, W. K., Shelley, E. G., Haerendel, G. & Paschmann, G. 1982 Energetic ion composition in the subsolar magnetopause and boundary layer. *J. geophys. Res.* **87**, 2139.
- Petschek, H. E. 1964 Magnetic field annihilation. *NASA Special Publ.* **SP-50**, 425.
- Pudovkin, M. I. & Semenov, V. S. 1985 Magnetic field reconnection theory and the solar-wind-magnetosphere interaction: a review. *Space Sci. Rev.* **41**, 1.
- Rijnbeek, R. P. 1984 Impulsive reconnection signatures at the Earth's magnetopause. Ph.D. thesis, Imperial College, London.
- Rijnbeek, R. P., Biernat, H. K., Heyn, M. F., Farrugia, C. J., Southwood, D. J., Paschmann, G., Sckopke, N. & Russell, C. T. 1989 The structure of the reconnection layer observed by *ISEE 1* on 8 September 1978. (In the press.)
- Rijnbeek, R. P., Cowley, S. W. H., Southwood, D. J. & Russell, C. T. 1984a A survey of dayside flux transfer events observed by *ISEE 1* and 2 magnetometers. *J. geophys. Res.* **89**, 786.
- Rijnbeek, R. P., Cowley, S. W. H., Southwood, D. J. & Russell, C. T. 1984b Recent investigations of flux transfer events observed at the dayside magnetopause. In *Magnetic Reconnection in Space and Laboratory Plasmas* (ed. E. W. Hones Jr) Washington, D.C.: American Geophysical Union.
- Rijnbeek, R. P., Farrugia, C. J., Southwood, D. J., Dunlop, M. W., Mier-Jedrzejowicz, W. A. C., Chaloner, C. P., Hall, D. S. & Smith, M. F. 1987 A magnetic boundary signature within flux transfer events. *Planet. Space Sci.* **35**, 871.
- Russell, C. T. & Elphic, R. C. 1978 Initial *ISEE* magnetometer results: magnetopause observations. *Space Sci. Rev.* **22**, 681-715.
- Saunders, M. A., Russell, C. T. & Sckopke, N. 1984a Flux transfer events: scale size and interior structure. *Geophys. Res. Lett.* **11**, 131.
- Saunders, M. A., Russell, C. T. & Sckopke, N. 1984b A dual-satellite study of the spatial properties of FTEs. In *Magnetic Reconnection in Space and Laboratory Plasmas* (ed. E. W. Hones Jr) Washington, D.C.: American Geophysical Union.
- Semenov, V. S., Kubyshleni, I. V., Heyn, M. F. & Biernat, H. K. 1984 Temporal evolution of the convective plasma flow during a reconnection process. *Adv. Space Res.* **4**, 471.
- Sonnerup, B. U. O., Paschmann, G., Papamastorakis, I., Sckopke, N., Haerendel, G., Bame, S. J., Asbridge, J. R., Gosling, J. T. & Russell, C. T. 1981 Evidence for magnetic field reconnection at the Earth's magnetopause. *J. geophys. Res.* **86**, 10049.
- Southwood, D. J. 1985 Theoretical aspects of ionosphere-magnetosphere-solar-wind coupling. In *Physics of Ionosphere-Magnetosphere*. *Adv. Space Res.* **5**, 4-7.
- Southwood, D. J., Farrugia, C. J. & Saunders, M. A. 1988 What are flux transfer events? *Planet. Space Sci.* **36**, 503.
- Southwood, D. J., Saunders, M. A., Dunlop, M. W., Mier-Jedrzejowicz, W. A. C. & Rijnbeek, R. P. 1986 A survey of flux transfer events recorded by the *UKS* spacecraft magnetometer. *Planet. Space Sci.* **34**, 1349-1359.

Discussion

S. SCHWARTZ (*Queen Mary College, London, U.K.*). If the spacecraft passes through an FTE while unsteady reconnection is still ongoing, would Dr Farrugia expect to see an asymmetry in the FTE signature, the reason being, for example, the exit from the FTE is closer to the diffusion region or slow shock?

C. J. FARRUGIA. At a speed of a few kilometres per second, a spacecraft is essentially a stationary observation point when one of those corrugations of the reconnection layer's boundary we drew sweeps past. The arrows indicating trajectories in figure 18 are in the rest frame of the 'bulge'. The spacecraft are, of course, moving predominantly outwards. Whether the spacecraft are closer to the diffusion region at the end of the FTE signature I do not know as this depends on the motion of the reconnection line. I do not therefore expect asymmetries in the sense that Dr Schwartz describes. I am not saying asymmetries are not observed. Farrugia *et al.* (1988) do report asymmetric observations as regards, for instance, electron intensities in the draping regions and wave emissions there. But I think these have a 'local' cause.

M. J. RYCROFT (*British Antarctic Survey, Cambridge, U.K.*). Does Dr Farrugia consider that waves, with frequencies above those at which magnetohydrodynamic waves propagate, are important in the processes which he has discussed?

C. J. FARRUGIA. Waves are a very effective means for redistributing energy and momentum in a collisionless plasma, and they can therefore influence the detailed evolution of the plasma in FTES. As regards their role in providing the anomalous resistivity required for reconnection, the view taken by LaBelle *et al.* (1987) on the waves observed is pessimistic because their power (concentrated at low frequencies) is low. In view of the small size of the diffusion region, it is possible that the waves associated with reconnection have not yet been observed. I think the state of the art is summarized well in a beautiful article by LaBelle & Treumann (1989).

D. A. BRYANT (*Rutherford Appleton Laboratory, Didcot, U.K.*). Further to Dr Farrugia's answer to Dr Rycroft's question, I think it is possible that waves, even at low power levels, could be important, if the reason for their low power is that wave energy is being absorbed as fast as it is being produced. Does Dr Farrugia agree?

C. J. FARRUGIA. I do agree, because then, by definition, the real power is greater than that observed. Once again, I refer Dr Bryant to LaBelle & Treumann's (1989) review article for a comprehensive discussion.

Additional reference

LaBelle, J. & Treumann, R. A. 1989 Plasma waves at the dayside magnetopause. (In the press.)